

S-D mixing and $\psi(3770)$ production in e^+e^- annihilation and B decay and its radiative transitions

Kui-Yong Liu

Department of Physics, Peking University, Beijing 100871, People's Republic of China and Department of Physics, Liaoning University, Shenyang 110036, People's Republic of China

Kuang-Ta Chao

China Center of Advanced Science and Technology (World Laboratory), Beijing 100080, People's Republic of China and Department of Physics, Peking University, Beijing 100871, People's Republic of China

Abstract

The large decay rate observed by Belle for $B^+ \rightarrow \psi(3770)K^+$, which is comparable to $B^+ \rightarrow \psi(3686)K^+$, might indicate either an unexpectedly large S-D mixing angle $|\theta| \approx 40^\circ$ or the leading role of the color-octet mechanism in D-wave charmonium production in B decay. By calculating the production rate of $\psi(3770)$ in the continuum e^+e^- annihilation at $\sqrt{s} = 10.6$ GeV with these two possible approaches (i.e. the large S-D mixing and the color-octet mechanism), we show that the measurement for this process at Belle and BaBar may provide a clear cut clarification for the two approaches. In addition, the radiative E1 transition ratio $\Gamma(\psi(3770) \rightarrow \gamma\chi_{c2})/\Gamma(\psi(3770) \rightarrow \gamma\chi_{c1})$ may dramatically change from ~ 0.04 (for $\theta \approx 0^\circ$) to ~ 200 (for $\theta \approx -40^\circ$) due to the large S-D interference effect, thus the E1 transition measurement of $\psi(3770)$ at BES and CLEO-c will also be very useful in clarifying this issue.

PACS number(s): 13.66.Bc, 14.40.Gx, 12.38.Bx

1 Introduction

The S-D mixing for $\psi' \equiv \psi(3686)$ and $\psi'' \equiv \psi(3770)$ is of great interest in charmonium physics. If we neglect the charmed meson pair component which is due to coupling to decay channels, ψ' and ψ'' may be approximately expressed as

$$|\psi'\rangle = \cos\theta |2^3S_1\rangle + \sin\theta |1^3D_1\rangle, \quad |\psi''\rangle = \cos\theta |1^3D_1\rangle + \sin\theta |2^3S_1\rangle. \quad (1)$$

A rough estimate of the S-D mixing angle may be obtained by using the ratio of the observed leptonic decay widths [1] of ψ' and ψ'' and neglecting the D-wave component contribution to these leptonic decay widths $\tan^2\theta = \frac{\Gamma(\psi'' \rightarrow l^+l^-)}{\Gamma(\psi' \rightarrow l^+l^-)} \approx 0.12$, which results in $\theta \approx \pm 19^\circ$. However, if the D-wave contribution to leptonic decay widths is further included, potential model calculations e.g. in [2, 3, 4] give two solutions: $\theta \approx -10^\circ$ to -13° or $\theta \approx +30^\circ$ to $+26^\circ$ ($\theta \approx -10^\circ$ and $+30^\circ$ in [2], $\theta \approx -13^\circ$ and $+26^\circ$ in [3], and $\theta \approx -12^\circ$ and $+27^\circ$ in [4]). The small mixing solution (i.e. $\theta \approx -10^\circ$) is compatible with the results obtained in models with coupled decay channels [5, 6]. Moreover, $\theta \approx -10^\circ$ is favored by the $\psi' \rightarrow \gamma\chi_{cJ}$ data whereas $\theta \approx +30^\circ$ would lead to $\Gamma(\psi' \rightarrow \gamma\chi_{c0}) \approx 135$ KeV due to a large positive S-D interference [3], which is higher than its observed value by a factor of 6 and is therefore disfavored. The S-D mixing may have many interesting phenomenological consequences. It might slightly [2] or substantially [7, 8] affect the $\psi(3770) \rightarrow J/\psi\pi\pi$ decay, which has been recently observed by

BES [9]. It would also have effects on the h_c search via the $\psi' \rightarrow h_c \pi^0$ decay [10]. The S-D mixing could even provide an explanation for the notorious $\rho\pi$ puzzle that the suppression of $\psi' \rightarrow \rho\pi$ is due to a destructive interference between the S and D wave states [4], and it might also be useful in explaining [11] the recent observed enhancement of $\psi' \rightarrow K_L K_S$ by BES [12]. Moreover, the ratio of $\frac{\Gamma(\psi(3770) \rightarrow \gamma \chi_{c2})}{\Gamma(\psi(3770) \rightarrow \gamma \chi_{c1})}$ may sensitively change from 0.04 (for $\theta \approx 0^\circ$) to 0.22 (for $\theta \approx -10^\circ$) and to 0.06 (for $\theta \approx +30^\circ$) [3]. The experimental examination of these radiative transitions for $\psi(3770)$ at BES and CLEO-c in the near future will be an interesting test for the S-D mixing.

Recently Belle Collaboration [13] has observed $\psi(3770)$ for the first time in the B meson decay $B^+ \rightarrow \psi(3770)K^+$ with a branching ratio of $(0.48 \pm 0.11 \pm 0.07) \times 10^{-3}$, which is comparable to $\mathcal{B}(B^+ \rightarrow \psi'(3686)K^+) = (0.66 \pm 0.06) \times 10^{-3}$ [1]. This is quite surprising, since conventionally $\psi(3770)$ and $\psi(3686)$ are regarded as mainly the 1^3D_1 and 2^3S_1 color-singlet $c\bar{c}$ states respectively, and the coupling of 1^3D_1 to the $c\bar{c}$ vector current in the weak decay effective hamiltonian is much weaker than that of 2^3S_1 . One possible explanation is that the S-D mixing for $\psi(3770)$ and $\psi(3686)$ is very large, much larger than previously expected. If in the B meson decay we neglect the 1^3D_1 contribution, which is expected to be much smaller than the 2^3S_1 contribution, we would get the S-D mixing angle $|\theta| \approx 40.4^\circ$ from the observed decay rate ratio

$$\frac{\mathcal{B}(B^+ \rightarrow \psi(3770)K^+)}{\mathcal{B}(B^+ \rightarrow \psi(3686)K^+)} = \tan^2 \theta \approx 0.73. \quad (2)$$

Although this large mixing angle seems to be not compatible with all our previous knowledge about the S-D mixing, it is still worthwhile to test it with new experiments. Another possible explanation is that the color-octet mechanism in nonrelativistic QCD (NRQCD) may play the leading role in the D-wave charmonium production in B meson decays, and it was predicted [14] that for a pure D-wave state the branching ratio $\mathcal{B}(B \rightarrow \psi(3770)X) \approx 0.28\%$, which is comparable to $\mathcal{B}(B \rightarrow \psi(3686)X) = (0.35 \pm 0.05)\%$ [1] (see also [15] for similar discussions). In a series of papers [16, 17, 14, 18] it was pointed out that based on the Fock state expansion and velocity scaling rules of NRQCD [19] the production rates of D-wave charmonium states including the 3D_1 $\psi(3770)$, which would predominantly decay to the $D\bar{D}$ meson pair, and an expected narrow 3D_2 state, which could have some decay fraction to $J/\psi\pi^+\pi^-$, would be comparable to that of J/ψ and $\psi(2S)$ in the Z^0 decay [16], the $p\bar{p}$ collision at the Tevatron [17], the B meson decay [14], and the fixed target experiments [18], whereas in the conventional color-singlet model the D-wave production rates, which are proportional to the squared second derivative of the $c\bar{c}$ wave function at the origin, should be greatly suppressed. Despite of certain uncertainties associated with the values of color-octet matrix elements, the color-octet contributions are expected to be dominant, which are larger than the color-singlet contributions by more than one order of magnitude in those processes. For instance, in the large p_T charmonium production at the Tevatron, the 3D_J states could have large rates, comparable to $\psi(2S)$, because in both cases the dominant production mechanism is expected to be gluon fragmentation into the color-octet 3S_1 $c\bar{c}$ intermediate state which then evolves respectively into the physical color-singlet 3D_J and $\psi(2S)$ states by emitting two soft gluons via double E1 transitions with the same order transition probabilities [17]. Similarly, the $\psi(3770)$ production in the B meson decay could provide another interesting test for the color-octet mechanism in NRQCD.

In order to distinguish between the large S-D mixing and the NRQCD color-octet mechanism in the $\psi(3770)$ production in the B meson decay, we suggest measuring the $\psi(3770)$ production in continuum e^+e^- annihilation at the Belle and BaBar energy $\sqrt{s} = 10.6$ GeV, and we will give calculations of the production cross sections in the following sections. We will show that the $\psi(3770)$ production in e^+e^- annihilation via double $c\bar{c}$ does not receive large contributions from the color-octet mechanism but is very sensitive to the S-D mixing.

J/ψ inclusive production in e^+e^- annihilation has been investigated within the color-singlet model [20] and the color-octet model [21, 22, 23]. BaBar [24] and Belle [25] have measured J/ψ production rate in continuum e^+e^- annihilations at $\sqrt{s} = 10.6$ GeV, which is found to be much larger than the color-singlet prediction. More interestingly, Belle further finds J/ψ production to be dominated by the double $c\bar{c}$ production [26]. The measured exclusive cross section for $e^+ + e^- \rightarrow J/\psi + \eta_c$ is an order of magnitude larger than the theoretical values[27], and the measured inclusive cross section for $e^+ + e^- \rightarrow J/\psi + c + \bar{c}$ is more than five times larger than NRQCD predictions. Therefore the inclusive charmonium production via double $c\bar{c}$ is particularly interesting and worth investigating. As in the case of inclusive production of J/ψ , η_c , and $\chi_{cJ}(J=0, 1, 2)$ [28], here we will also concentrate on the double $c\bar{c}$ production for the D-wave charmonium states $\delta_J(J = 1, 2, 3)$.

2 Color-singlet contribution to δ_1 (3D_1) charmonium production via double $c\bar{c}$ in e^+e^- annihilation

In NRQCD the Fock state expansion for the D-wave (without S-D mixing) charmonium $\delta_J(J = 1, 2, 3)$ is

$$\begin{aligned} |\delta_J\rangle &= O(1)|c\bar{c}(^3D_J, \underline{1})\rangle \\ &+ O(v)|c\bar{c}(^3P_J, \underline{8})g\rangle \\ &+ O(v^2)|c\bar{c}(^3S_1, \underline{8})gg\rangle + \dots \end{aligned} \quad (3)$$

Following the NRQCD factorization formalism, the scattering amplitude of the process $e^-(p_1) + e^+(p_2) \rightarrow \gamma^* \rightarrow c\bar{c}(^{2S+1}L_J^{(1,8a)})(p) + c(p_c) + \bar{c}(p_{\bar{c}})$ in Fig. 1 is given by

$$\begin{aligned} \mathcal{A}(e^-(p_1) + e^+(p_2) \rightarrow c\bar{c}(^{2S+1}L_J^{(1,8a)})(p) + c(p_c) + \bar{c}(p_{\bar{c}})) &= \sqrt{C_L} \sum_{L_z S_z} \sum_{s_1 s_2} \sum_{jk} \\ &\times \langle s_1; s_2 | SS_z \rangle \langle LL_z; SS_z | JJ_z \rangle \langle 3j; \bar{3}k | 1, 8a \rangle \\ &\times \begin{cases} \mathcal{A}(e^-(p_1) + e^+(p_2) \rightarrow c_j(\frac{p}{2}; s_1) + \bar{c}_k(\frac{p}{2}; s_2) + c_l(\frac{p_c}{2}; s_3) + \bar{c}_i(\frac{p_{\bar{c}}}{2}; s_4)) & (L = S), \\ \epsilon_\alpha^*(L_z) \mathcal{A}^\alpha(e^-(p_1) + e^+(p_2) \rightarrow c_j(\frac{p}{2}; s_1) + \bar{c}_k(\frac{p}{2}; s_2) + c_l(\frac{p_c}{2}; s_3) + \bar{c}_i(\frac{p_{\bar{c}}}{2}; s_4)) & (L = P), \\ \frac{1}{2} \epsilon_{\alpha\beta}^*(L_z) \mathcal{A}^{\alpha\beta}(e^-(p_1) + e^+(p_2) \rightarrow c_j(\frac{p}{2}; s_1) + \bar{c}_k(\frac{p}{2}; s_2) + c_l(\frac{p_c}{2}; s_3) + \bar{c}_i(\frac{p_{\bar{c}}}{2}; s_4)) & (L = D). \end{cases} \end{aligned} \quad (4)$$

where $c\bar{c}(^{2S+1}L_J^{(1,8a)})$ is the $c\bar{c}$ pair produced at short distances, which subsequently evolve into a specific charmonium state at long distances, \mathcal{A}^α and $\mathcal{A}^{\alpha\beta}$ are the derivatives of the amplitude with respect to the relative momentum between the quark and anti-quark in the bound state. For the case of color-singlet state, the coefficient C_L can be related to the origin

of the radial wave function (or its derivatives) of the bound state as

$$C_D = \frac{15}{8\pi} |R_D''(0)|^2. \quad (5)$$

The spin projection operators and their derivatives with respect to the relative momentum are

$$P_{1S_z}(p, 0) = \frac{1}{2\sqrt{2}} \not{\epsilon}(S_z)(\not{p} + 2m_c), \quad (6)$$

$$P_{1S_z}^\alpha(p, 0) = \frac{1}{4\sqrt{2}m_c} [\gamma^\alpha \not{\epsilon}^*(S_z)(\not{p} + 2m_c) - (\not{p} - 2m_c) \not{\epsilon}(S_z)\gamma^\alpha]. \quad (7)$$

$$P_{1S_z}^{\alpha\beta}(p, 0) = \frac{1}{2\sqrt{2}m_c} [\gamma^\alpha \not{\epsilon}^*(S_z)\gamma^\beta + \gamma^\beta \not{\epsilon}(S_z)\gamma^\alpha]. \quad (8)$$

The calculation of cross sections for $e^- + e^+ \rightarrow \gamma^* \rightarrow \text{charmonium} + c\bar{c}$ is straightforward. As in Ref. [20] we write the differential cross section as

$$\frac{d\sigma(e^+ + e^- \rightarrow \gamma^* \rightarrow \text{charmonium} + c\bar{c})}{dz} = \frac{4C_D\alpha^2\alpha_s^2}{81m_c} (S(z) + \frac{\alpha(z)}{3}). \quad (9)$$

where $z = 2E_\psi/\sqrt{s}$. The expressions of $S(z)$ and $\alpha(z)$ for δ_J are lengthy and will be given in the appendix for $J = 1, 2$. With Eq. (9) we can evaluate the inclusive cross sections for δ_J . The input parameters used in the numerical calculations are

$$m_c = 1.5\text{GeV}, \quad \alpha_s(2m_c) = 0.26, \quad \alpha = 1/137, \quad |R_D''(0)|^2 = 0.015\text{GeV}^7 [29]. \quad (10)$$

and the obtained cross section for the δ_1 at $\sqrt{s} = 10.6$ GeV is

$$\sigma(e^+ + e^- \rightarrow \gamma^* \rightarrow \delta_1 + c\bar{c}) = 2.5 \text{ fb}. \quad (11)$$

Here we also give the calculated cross section for the δ_2 at $\sqrt{s} = 10.6$ GeV

$$\sigma(e^+ + e^- \rightarrow \gamma^* \rightarrow \delta_2 + c\bar{c}) = 2.4 \text{ fb}. \quad (12)$$

We also find that as in the case of other charmonium states [28] the calculated cross sections for δ_1 in eq. (11) and δ_2 in eq. (12) are substantially smaller than those obtained in the fragmentation approximation at $\sqrt{s} = 10.6$ GeV which would cause an enhancement factor of 1.5 and 2.3 respectively.

Comparing eq.(11) with $\sigma(e^+ + e^- \rightarrow \gamma^* \rightarrow J/\psi + c\bar{c}) = 148 \text{ fb}$ calculated for the J/ψ in [28], we see that the inclusive double $c\bar{c}$ cross section for the D-wave 1^{--} state is smaller than that for the S-wave 1^{--} states by a factor of 60. This illustrates the expectation that within the color-singlet model the suppression of D-wave state production relative to the S-wave state production is usually about two orders of magnitude.

3 Color-octet contribution to δ_1 production via double $c\bar{c}$ in e^+e^- annihilation

The color-octet contributions to δ_1 production via double $c\bar{c}$ in e^+e^- annihilation come from the Feynman diagrams in Fig 1 and Fig 2. According to the NRQCD factorization and velocity scaling rules[19], the contributions of the second term and third term in the Fock state expansion of δ_1 in eq. (3) are of the same order in the quark relative velocity v as the corresponding terms in the Fock state expansion of J/ψ or $\psi(2S)$. As a rough estimate for the nonperturbative matrix elements we may choose

$$\langle \mathcal{O}_8^{\delta_1}(^3S_1) \rangle \approx \langle \mathcal{O}_8^{J/\psi}(^3S_1) \rangle = 1.06 \times 10^{-2} \text{ GeV}^3, \quad (13)$$

$$\langle \mathcal{O}_8^{\delta_1}(^3P_0) \rangle / m_c^2 \approx \langle \mathcal{O}_8^{J/\psi}(^3P_0) \rangle / m_c^2 = 1.1 \times 10^{-2} \text{ GeV}^3, \quad (14)$$

$$\langle \mathcal{O}_8^{\delta_1}(^1S_0) \rangle \ll \langle \mathcal{O}_8^{J/\psi}(^1S_0) \rangle = 3.3 \times 10^{-2} \text{ GeV}^3, \quad (15)$$

$$\langle \mathcal{O}_8^H(^3P_J) \rangle = (2J+1) \langle \mathcal{O}_8^H(^3P_0) \rangle. \quad (16)$$

Here the color-octet matrix elements for J/ψ were extracted from the J/ψ data at the Tevatron (see Ref. [33, 34] for detailed discussions). There are large uncertainties with $\langle \mathcal{O}_8^{J/\psi}(^3P_0) \rangle / m_c^2$ and $\langle \mathcal{O}_8^{J/\psi}(^1S_0) \rangle / 3$ and their combinations, and here we have assumed that they are equal and take the largest fitted values from [33] to avoid underestimates of the color-octet contributions. (note that these two matrix elements may be overestimated [34].)

In Fig. 1, the color-octet contribution can be obtained from the corresponding color-singlet contribution divided by a factor of $\frac{32\langle \mathcal{O}_8^H(^{2S+1}L_J) \rangle}{3\langle \mathcal{O}_8^H(^{2S+1}L_J) \rangle}$. With the matrix elements for $\langle \mathcal{O}_8^{\delta_1}(^{2S+1}L_J) \rangle$ chosen above, we find the contributions to δ_1 production cross section from the color-octet $^3S_1, ^3P_0, ^3P_1, ^3P_2$ states to be 0.12fb, 1.1fb, 0.29fb, 0.14fb respectively. The total color-octet contribution to the cross section from Fig. 1 is 1.65fb.

In Fig. 2 the color-octet contributions come from four different (the upper two and the lower two) diagrams. The upper diagrams only contribute via the color-octet 3S_1 state, and the differential cross section reads

$$\frac{d\sigma_{octet}}{dz} = \frac{16\alpha^2\alpha_s^2 \langle \mathcal{O}_8^{\delta_1}(^3S_1) \rangle}{27m_c} |\bar{M}|^2, \quad (17)$$

where $|\bar{M}|^2$ takes the form

$$\begin{aligned} |\bar{M}|^2 = & \frac{\pi}{12\delta^2 s^2 z(z-2)^2} \left\{ -4z \sqrt{\frac{(1-z)(z^2-\delta^2)}{4+\delta^2-4z}} \right. \\ & [3\delta^4 - 12\delta^2(z-2) + 16(10+z(z-10))] + \\ & (z-2)^2 [3\delta^4 - 8\delta^2(3z-4) + 32(2+z(z-2))] \\ & \left. \ln \left[\frac{z\sqrt{4+\delta^2-4z} + 2\sqrt{(1-z)(z^2-\delta^2)}}{z\sqrt{4+\delta^2-4z} - 2\sqrt{(1-z)(z^2-\delta^2)}} \right] \right\}. \quad (18) \end{aligned}$$

The numerical result for the cross section is

$$\sigma_{octet}(e^+e^- \rightarrow \delta_1 c\bar{c}) = 4.5 \text{ fb.} \quad (19)$$

The lower diagrams in Fig. 2 make contributions to δ_1 production via the color-octet ${}^3P_J (J = 0, 1, 2)$ and 1S_0 intermediate states. We find the following results.

$$\frac{d\sigma_{octet}}{dz} = \frac{32\alpha^2\alpha_s^2 \langle \mathcal{O}_8^{\delta_1}(2S+1L_J) \rangle}{27m_c} \sqrt{\frac{(z^2 - \delta^2)(1-z)}{4 + \delta^2 - 4z}} |\bar{M}({}^{2S+1}L_J)|^2, \quad (20)$$

$$|\bar{M}({}^3P_0)|^2 = \frac{(16\pi(8 + 3\delta^2 - 8z)(\delta^6 + 8\delta^2(-4 + z)z^2 + 8z^4 + 2\delta^4(18 + (-10 + z)z)))}{(27\delta^2s^3(4 + \delta^2 - 4z)^2(-2 + z)^4)} \quad (21)$$

$$\begin{aligned} |\bar{M}({}^3P_1)|^2 &= \frac{1}{(9\delta^2s^3(4 + \delta^2 - 4z)^2(-2 + z)^4)} \\ &\times (16\pi(8 + 3\delta^2 - 8z)(\delta^6 + 16(-2 + z)^2z^2 + 2\delta^4(18 + (-12 + z)z) \\ &- 4\delta^2(-2 + z)(16 + z(-20 + 3z)))) \end{aligned} \quad (22)$$

$$|\bar{M}({}^3P_2)|^2 = \frac{(32\pi(8 + 3\delta^2 - 8z)(\delta^6 + 2\delta^4(-3 + z)(-2 + z) + 4z^4 - 2\delta^2z^2(2 + z)))}{(9\delta^2s^3(4 + \delta^2 - 4z)^2(-2 + z)^4)} \quad (23)$$

$$|\bar{M}({}^1S_0)|^2 = \frac{(-8\pi(8 + 3\delta^2 - 8z)(\delta - z)(\delta + z))}{(9s^2(4 + \delta^2 - 4z)^2(-2 + z)^2)} \quad (24)$$

With the chosen parameters mentioned above, the contributions to the $\delta_1 c\bar{c}$ production cross section come from the color-octet 3P_0 , 3P_1 and 3P_2 are 0.18fb, 2.7fb and 0.87fb respectively. The contribution of the color-octet 1S_0 is negligible.

The total color-octet contribution to the cross section from Fig. 2 is 8.3fb, and the sum of the color-octet contributions from Fig. 1 and Fig. 2 is 9.9fb. This number could become substantially smaller if we use the matrix element values given in [34]. In any case, the color-octet contribution to the D-wave states production cross sections should be of the same order as the color-singlet contribution, because from the δ_J Fock state expansion in eq.(3) and from Fig. 1 and Fig. 2 it is easy to see that the color-octet and color-singlet contributions are of the same order in both short distance ($O(\alpha_s^2)$) and long distance ($O(v^4)$) parts. Based on the above calculations including both the color-singlet and color-octet contributions, we think

$$\sigma(e^+ + e^- \rightarrow \gamma^* \rightarrow \delta_1 + c\bar{c}) \approx 10 \text{ fb} \quad (25)$$

should be a reasonable estimate in NRQCD for the $\psi(3770)$ production rate when the S-D mixing is neglected.

4 S-D mixing and $\psi(3770)$ production in e^+e^- annihilation and B decay

The calculated $\psi(3770)c\bar{c}$ production rate could be significantly enhanced by the S-D mixing if the mixing angle is large. With the calculated J/ψ production cross section $\sigma(e^+ + e^- \rightarrow \gamma^* \rightarrow J/\psi + c\bar{c}) = 148 \text{ fb}$ [28], the $\psi(2S)$ production cross section can be approximately obtained by the scale factor $|R_{2S}(0)|^2 / |R_{1S}(0)|^2$, and then we have $\sigma(e^+ + e^- \rightarrow \gamma^* \rightarrow \psi(2S) + c\bar{c}) = 90 \text{ fb}$ (the color-octet contributions to the S-wave charmonia are small and negligible). If this estimate for the $\psi(2S)$ makes sense, with the large S-D mixing angle $\theta \approx \pm 40^\circ$ we would have

$$\sigma(e^+ + e^- \rightarrow \psi(3770) + c\bar{c}) \approx \sigma(e^+ + e^- \rightarrow \psi(2S) + c\bar{c}) \times \tan^2 \theta \approx 66 \text{ fb}. \quad (26)$$

This value is much larger than 10 fb, the value in eq.(25) obtained without S-D mixing in NRQCD.

However, as we already mentioned, the Belle observed double charm production cross section for the J/ψ has a much higher value[26]

$$\sigma(e^+ + e^- \rightarrow J/\psi + c\bar{c}) = (0.87 \pm 0.15 \pm 0.12) \text{ pb}, \quad (27)$$

which is larger than the theoretical expectation in NRQCD by a factor of 6 (as a rough estimate we neglect the feed down contribution from the $\psi(2S)$ and χ_{cJ} states in the J/ψ production cross section). If this also happens for the $\psi(2S)$, which is very likely, we would expect

$$\sigma(e^+ + e^- \rightarrow \psi(2S) + c\bar{c}) \approx 530 \text{ fb} \quad (28)$$

to be the observed double charm production cross section for the $\psi(2S)$. Then with the large S-D mixing angle $\theta \approx \pm 40^\circ$ we would have

$$\sigma(e^+ + e^- \rightarrow \psi(3770) + c\bar{c}) \approx \sigma(e^+ + e^- \rightarrow \psi(2S) + c\bar{c}) \times \tan^2 \theta \approx 387 \text{ fb}. \quad (29)$$

This is more than an order of magnitude larger than the value in eq.(25) obtained without S-D mixing in NRQCD.

In any case, we see that the large S-D mixing angle $\theta \approx \pm 40^\circ$ would result in a much higher cross section for the $\psi(3770)$ double charm production than that without S-D mixing or with small S-D mixing angle like $\theta \approx -10^\circ$. This is due to the fact that the double charm production rate for a pure 2^3S_1 state is much higher than that for a pure 1^3D_1 state in NRQCD. We therefore suggest measuring the production cross sections of $\psi(3770) + c\bar{c}$ and $\psi(3686) + c\bar{c}$ in the continuum e^+e^- annihilation at $\sqrt{s} = 10.6 \text{ GeV}$ by Belle and BaBar.

In contrast, in the B inclusive decay to $\psi(3770)$, the decay rate is expected to be insensitive to the S-D mixing in NRQCD, because both the 2^3S_1 and 1^3D_1 final states produced in B decay are dominated by the color-octet intermediate states with the same quantum numbers in the two cases and thus they may have comparable production rates. The color-octet dominance in B decay relies on two observations. The first is that in the effective weak interactions the squared short distance coefficient at the b quark mass scale for the color-octet part is larger than that for the color-singlet part by more than an order of magnitude. The second is that the color-singlet S-wave contribution is further suppressed by QCD radiative

corrections and therefore negligible (see [35][36][37] for detailed discussions). Therefore, despite of certain uncertainties related to the values of color-octet matrix elements and other parameters, the qualitative features for the D-wave charmonium production in e^+e^- annihilation and B decay should hold and be tested.

5 S-D mixing and $\psi(3770)$ E1 transitions

As mentioned already, the small S-D mixing angle like $\theta \approx -10^\circ$ is favored by the observed E1 transition rates of $\psi(3686)$. However, as another independent check for the mixing angle, measurements on the $\psi(3770)$ E1 transitions will be also very useful. In ref.[3] the E1 transition rates of $\psi(3770)$ were calculated for $\theta = 0^\circ, -10^\circ, +30^\circ$, and the S-D interference effects were found to be significant. Based on the same potential model we now estimate the E1 transition widths for $\theta = \pm 40.4^\circ$ and find

$$\Gamma(\psi(3770) \rightarrow \gamma\chi_{cJ}) = 386, 0.32, 66 \text{ KeV} \quad (30)$$

for $J=0,1,2$ with $\theta = -40.4^\circ$; and

$$\Gamma(\psi(3770) \rightarrow \gamma\chi_{cJ}) = 52, 203, 28 \text{ KeV} \quad (31)$$

for $J=0,1,2$ with $\theta = +40.4^\circ$.

We see that the S-D interference effects in the $\psi(3770)$ E1 transitions are essential. In particular, the ratio

$$R_{2/1} = \frac{\Gamma(\psi(3770) \rightarrow \gamma\chi_{c2})}{\Gamma(\psi(3770) \rightarrow \gamma\chi_{c1})} \quad (32)$$

will dramatically change from ~ 0.04 (for $\theta \approx 0^\circ$) to ~ 200 (for $\theta \approx -40^\circ$) due to the large S-D interference effect. Similar discussions for $\theta \approx -12^\circ$ and $+27^\circ$ can also be found in [4].

We hope these measurements can be performed at BES and CLEO-c in the near future. They will be very helpful in clarifying the S-D mixing problem for $\psi(3770)$ and $\psi(3686)$.

6 Discussions and summary

We first discuss about the uncertainties associated with the color-octet matrix elements with different choices from eqs.(13)-(15). According to the NRQCD velocity scaling rules, we may have

$$\langle \mathcal{O}_1^{\delta J}(^3D_J) \rangle \sim m_c^7 v^7, \quad \langle \mathcal{O}_8^{\delta J}(^3P_1) \rangle \sim m_c^5 v^7, \quad \langle \mathcal{O}_8^{\delta J}(^3S_1) \rangle \sim m_c^3 v^7. \quad (33)$$

If we use $\langle \mathcal{O}_1^{\delta 1}(^3D_1) \rangle$ as the input parameter, $\langle \mathcal{O}_1^{\delta 1}(^3D_1) \rangle = \frac{45N_c}{4\pi} |R_D''(0)|^2 = 0.16 \text{ GeV}^7$, we would have the following matrix elements

$$\frac{\langle \mathcal{O}_1^{\delta 1}(^3D_1) \rangle}{m_c^7} \approx \frac{\langle \mathcal{O}_8^{\delta 1}(^3P_1) \rangle}{m_c^5} \approx \frac{\langle \mathcal{O}_8^{\delta 1}(^3S_1) \rangle}{m_c^3} = 0.0094. \quad (34)$$

Then the color-octet contributions to the cross section $\sigma(e^+e^- \rightarrow ({}^{2S+1}L_J^{(8)}) + c\bar{c} \rightarrow \delta_1 + c\bar{c})$ can be estimated to be 0.36 fb, 1.1 fb, 0.28 fb, 0.12 fb for ${}^3S_1^{(8)}, {}^3P_0^{(8)}, {}^3P_1^{(8)}, {}^3P_2^{(8)}$ color-octet

intermediate states respectively from Fig. 1; and 13.5 fb, 0.17 fb, 2.6 fb, 0.83 fb respectively from Fig. 2. The total contribution to the cross section $\sigma(e^+e^- \rightarrow \gamma^* \rightarrow \delta_1 + c\bar{c})$ is about 20 fb, a factor of 2 larger than 10 fb, the value given in eq.(25) obtained by using eqs.(13)-(15). The above results may demonstrate the possible uncertainties associated with the color-octet matrix elements, which are estimated according to the NRQCD velocity scaling rules but with different choices for the input parameters. We expect that these uncertainties do not change our main analysis that the $\psi(3770)$ production in e^+e^- annihilation receives much smaller contributions from the color-octet channels than from the large S-D mixing.

We suggest performing the measurements on the $\psi(2S)$ and $\psi(3770)$ production in the continuum e^+e^- annihilation by Belle and BaBar in order to check (i) if the $\psi(2S) + c\bar{c}$ cross section is as large as about 0.5pb, which would confirm the S-wave (not only for 1S but also for 2S) charmonium production enhancement via double $c\bar{c}$; (ii) if the cross section of $\psi(3770) + c\bar{c}$ is comparable to that of $\psi(2S) + c\bar{c}$, which would confirm the large S-D mixing angle; (iii) if the cross section of $\psi(3770) + c\bar{c}$ is as small as say 10 fb, which would favor the prediction in NRQCD. It is very likely that Belle and BaBar will find a strong signal for $\psi(2S) + c\bar{c}$, because experimentally Belle has found a large cross section for the inclusive $\psi(2S) + X$ cross section, which is comparable to that for $J/\psi + X$ [25]. If a large $\psi(2S) + c\bar{c}$ cross section turned out to be the case, then one can easily distinguish between the large S-D mixing and the NRQCD prediction (together with the small S-D mixing) by simultaneously measuring the $\psi(3770) + c\bar{c}$ cross section.

In conclusion, we notice that the large decay rate observed by Belle for $B^+ \rightarrow \psi(3770)K^+$, which is comparable to $B^+ \rightarrow \psi(3686)K^+$, might indicate either an unexpectedly large S-D mixing angle $|\theta| \approx 40^\circ$ or the leading role of the color-octet mechanism in D-wave charmonium production in B decay. By calculating the production rate of $\psi(3770)$ in the continuum e^+e^- annihilation at $\sqrt{s} = 10.6$ GeV with these two possible approaches (i.e. the large S-D mixing and the color-octet mechanism), we show that the measurement for this process at Belle and BaBar may provide a clear cut clarification for the two approaches. In addition, the radiative E1 transition ratio $\Gamma(\psi(3770) \rightarrow \gamma\chi_{c2})/\Gamma(\psi(3770) \rightarrow \gamma\chi_{c1})$ may dramatically change from ~ 0.04 (for $\theta \approx 0^\circ$) to ~ 200 (for $\theta \approx -40^\circ$) due to the large S-D interference effect, thus the E1 transition measurement of $\psi(3770)$ at BES and CLEO-c will also be very useful in clarifying this issue.

Acknowledgments

We thank Z.G.He and Y.J.Zhang for help in checking some of the calculations. This work was supported in part by the National Natural Science Foundation of China, the Education Ministry of China, and the Beijing Electron Positron Collider National Laboratory.

Appendix

In this appendix, for δ_1 and δ_2 we give the expressions of $S(z)$ and $\alpha(z)$ which are defined in Eq. (9).

$$\begin{aligned}
S_{\delta_1} = & \frac{16\pi}{225\delta^6 s^4 (\delta - z)(-2 + z)^{10} z^7 (\delta + z)} \left\{ -4z \sqrt{\frac{(1-z)(z^2 - \delta^2)}{4 + \delta^2 - 4z}} \right. \\
& \times [-5529600\delta^{12} - 1382400\delta^{14} + (42393600\delta^{10} + 38246400\delta^{12} + 5529600\delta^{14})z \\
& - (124600320\delta^8 + 260259840\delta^{10} + 109255680\delta^{12} + 10114560\delta^{14})z^2 \\
& + (145981440\delta^6 + 702873600\delta^8 + 687037440\delta^{10} + 175499520\delta^{12} \\
& + 10955520\delta^{14})z^3 - (106168320\delta^4 + 732979200\delta^6 + 1706803200\delta^8 \\
& + 1037391360\delta^{10} + 178859520\delta^{12} + 7741440\delta^{14})z^4 + (483655680\delta^4 \\
& + 1502760960\delta^6 + 2324674560\delta^8 + 992090880\delta^{10} + 121618560\delta^{12} \\
& + 3672000\delta^{14})z^5 - (106168320\delta^2 + 759152640\delta^4 + 1448421376\delta^6 \\
& + 1866987008\delta^8 + 606618880\delta^{10} + 54528192\delta^{12} + 1110144\delta^{14})z^6 \\
& + (524943360\delta^2 + 98590720\delta^4 + 329316352\delta^6 + 803530752\delta^8 + 221747328\delta^{10} \\
& + 15245760\delta^{12} + 188688\delta^{14})z^7 + (70778880 - 1436221440\delta^2 + 1035042816\delta^4 \\
& + 448612352\delta^6 - 146389760\delta^8 - 42081920\delta^{10} - 2067024\delta^{12} + 26616\delta^{14})z^8 \\
& - (566231040 - 2742845440\delta^2 + 1070004224\delta^4 + 82320896\delta^6 - 4038536\delta^8 \\
& - 73280\delta^{10} + 262944\delta^{12} + 3180\delta^{14})z^9 + (2235432960 - 3145580544\delta^2 \\
& + 493045760\delta^4 - 287114752\delta^6 - 34498880\delta^8 + 1811280\delta^{10} - 41160\delta^{12} \\
& + 630\delta^{14})z^{10} - (5315624960 - 1154056192\delta^2 + 773548544\delta^4 - 101372288\delta^6 \\
& - 12039424\delta^8 - 258940\delta^{10} + 5445\delta^{12})z^{11} + (8075444224 + 1656672256\delta^2 \\
& + 1123221504\delta^4 + 50333664\delta^6 - 1196496\delta^8 + 110862\delta^{10} - 315\delta^{12})z^{12} \\
& - (8028487680 + 2410575872\delta^2 + 723781760\delta^4 + 38182256\delta^6 + 791960\delta^8 \\
& - 795\delta^{10})z^{13} + (5278310400 + 1389795328\delta^2 + 236564032\delta^4 + 8583048\delta^6 \\
& + 16302\delta^8)z^{14} - (2310758400 + 445429248\delta^2 + 39874240\delta^4 + 590984\delta^6)z^{15} \\
& + (673812480 + 84606976\delta^2 + 3518976\delta^4)z^{16} - (124616704 + 9082368\delta^2)z^{17} \\
& + 11939840z^{18}] + 15\delta^2(z - 2)^4 \ln \left[\frac{z\sqrt{4 + \delta^2 - 4z} + 2\sqrt{(1-z)(z^2 - \delta^2)}}{z\sqrt{4 + \delta^2 - 4z} - 2\sqrt{(1-z)(z^2 - \delta^2)}} \right] \\
& \times [23040\delta^{12} - (176640\delta^{10} + 69120\delta^{12})z + (519168\delta^8 + 585984\delta^{10} \\
& + 89856\delta^{12})z^2 - (608256\delta^6 + 1620480\delta^8 + 799296\delta^{10} + 63936\delta^{12})z^3 \\
& + (442368\delta^4 + 1380864\delta^6 + 1912960\delta^8 + 578944\delta^{10} + 26880\delta^{12})z^4 \\
& - (724992\delta^4 + 378112\delta^6 + 924480\delta^8 + 227248\delta^{10} + 6144\delta^{12})z^5 \\
& - (1032192\delta^2 + 256000\delta^4 + 1437696\delta^6 + 22176\delta^8 - 46976\delta^{10} - 1056\delta^{12})z^6 \\
& + (2310144\delta^2 + 503808\delta^4 + 1262528\delta^6 + 108816\delta^8 - 11916\delta^{10} - 252\delta^{12})z^7 \\
& - (229376\delta^2 - 856576\delta^4 - 194944\delta^6 - 29976\delta^8 - 3592\delta^{10} - 42\delta^{12})z^8 \\
& + (294912 - 3428352\delta^2 - 1397248\delta^4 - 571184\delta^6 - 25516\delta^8 - 447\delta^{10})z^9
\end{aligned}$$

$$\begin{aligned}
& - (1392640 - 4259840\delta^2 - 583680\delta^4 - 215072\delta^6 - 3078\delta^8 + 21\delta^{10})z^{10} \\
& + (1998848 - 2720768\delta^2 + 20736\delta^4 - 16052\delta^6 + 345\delta^8)z^{11} \\
& - (1163264 - 1031936\delta^2 + 98816\delta^4 + 3554\delta^6)z^{12} + (284672 - 172800\delta^2 \\
& + 22288\delta^4)z^{13} - (35840 - 5376\delta^2)z^{14} + 4096z^{15} \}. \tag{35}
\end{aligned}$$

$$\begin{aligned}
\alpha_{\delta_1} = & \frac{16\pi}{225\delta^6 s^4 (\delta - z)(-2 + z)^{10} z^7 (\delta + z)} \left\{ -4z \sqrt{\frac{(1-z)(z^2 - \delta^2)}{4 + \delta^2 - 4z}} \right. \\
& \times [5529600\delta^{12} + 1382400\delta^{14} - (46080000\delta^{10} + 39168000\delta^{12} + 5529600\delta^{14})z \\
& + (124600320\delta^8 + 248832000\delta^{10} + 105477120\delta^{12} + 10114560\delta^{14})z^2 \\
& - (48660480\delta^6 + 613171200\delta^8 + 574632960\delta^{10} + 155262720\delta^{12} \\
& + 10955520\delta^{14})z^3 + (35389440\delta^4 + 78028800\delta^6 + 1309163520\delta^8 \\
& + 755489280\delta^{10} + 140951040\delta^{12} + 7741440\delta^{14})z^4 - (117964800\delta^4 \\
& - 359485440\delta^6 + 1567180800\delta^8 + 620524800\delta^{10} + 82139520\delta^{12} \\
& + 3672000\delta^{14})z^5 + (318504960\delta^2 + 290734080\delta^4 - 1587570688\delta^6 \\
& + 1071024640\delta^8 + 324301568\delta^{10} + 29522496\delta^{12} + 1110144\delta^{14})z^6 \\
& - (1032192000\delta^2 + 235642880\delta^4 - 3195049984\delta^6 + 256432128\delta^8 \\
& + 97444224\delta^{10} + 4799424\delta^{12} + 188688\delta^{14})z^7 - (-70778880 + 276234240\delta^2 \\
& + 1370357760\delta^4 + 4314056704\delta^6 + 282550016\delta^8 - 6669952\delta^{10} + 647376\delta^{12} \\
& + 26616\delta^{14})z^8 + (-566231040 + 6529515520\delta^2 + 4711155712\delta^4 \\
& + 4188711424\delta^6 + 355571200\delta^8 + 6214976\delta^{10} + 832320\delta^{12} + 3180\delta^{14})z^9 \\
& - (-2235432960 + 14312718336\delta^2 + 6829299712\delta^4 + 2844373504\delta^6 \\
& + 199898048\delta^8 + 4164432\delta^{10} + 42696\delta^{12} + 630\delta^{14})z^{10} + (-5315624960 \\
& + 15998746624\delta^2 + 5588809216\delta^4 + 1329557888\delta^6 + 74936896\delta^8 \\
& + 265900\delta^{10} + 19515\delta^{12})z^{11} - (-8075444224 + 10653200384\delta^2 \\
& + 2855909376\delta^4 + 440017440\delta^6 + 16253328\delta^8 + 284850\delta^{10} + 315\delta^{12})z^{12} \\
& + (-8028487680 + 4372645888\delta^2 + 953109376\delta^4 + 93564688\delta^6 \\
& + 3276232\delta^8 + 795\delta^{10})z^{13} + (5278310400 - 1039542272\delta^2 - 183272384\delta^4 \\
& - 12182904\delta^6 + 16302\delta^8)z^{14} - (2310758400 - 70162944\delta^2 - 11162432\delta^4 \\
& + 590984\delta^6)z^{15} + (673812480 + 33531904\delta^2 + 3518976\delta^4)z^{16} \\
& - (124616704 + 9082368\delta^2)z^{17} + 11939840z^{18}] \\
& - 15\delta^2(-2 + z)^4 \ln \left[\frac{z\sqrt{4 + \delta^2 - 4z} + 2\sqrt{(1-z)(z^2 - \delta^2)}}{z\sqrt{4 + \delta^2 - 4z} - 2\sqrt{(1-z)(z^2 - \delta^2)}} \right] \\
& \times [23040\delta^{12} - (192000\delta^{10} + 69120\delta^{12})z + (519168\delta^8 + 507648\delta^{10} \\
& + 89856\delta^{12})z^2 - (202752\delta^6 + 1337856\delta^8 + 533952\delta^{10} + 63936\delta^{12})z^3 \\
& + (147456\delta^4 - 463360\delta^6 + 1415552\delta^8 + 245120\delta^{10} + 26880\delta^{12})z^4 \\
& - (61440\delta^4 - 2630912\delta^6 + 731072\delta^8 + 13136\delta^{10} + 6144\delta^{12})z^5 \\
& - (737280\delta^2 + 219136\delta^4 + 4452352\delta^6 - 169760\delta^8 + 38144\delta^{10} - 1056\delta^{12})z^6
\end{aligned}$$

$$\begin{aligned}
& + (835584\delta^2 - 724992\delta^4 + 3959872\delta^6 - 2256\delta^8 + 10380\delta^{10} - 252\delta^{12})z^7 \\
& - (1179648 - 3260416\delta^2 - 4187648\delta^4 + 1798528\delta^6 - 46024\delta^8 - 488\delta^{10} \\
& - 42\delta^{12})z^8 + (3244032 - 10629120\delta^2 - 7306752\delta^4 + 69936\delta^6 - 32804\delta^8 \\
& - 465\delta^{10})z^9 - (3031040 - 13373440\delta^2 - 6077440\delta^4 - 218592\delta^6 - 7418\delta^8 \\
& - 21\delta^{10})z^{10} + (950272 - 8346624\delta^2 - 2431744\delta^4 - 61164\delta^6 - 345\delta^8)z^{11} \\
& + (57344 + 2462976\delta^2 + 428416\delta^4 + 3554\delta^6)z^{12} - (63488 + 259328\delta^2 \\
& + 22288\delta^4)z^{13} + (17408 - 5376\delta^2)z^{14} - 4096z^{15}]. \tag{36}
\end{aligned}$$

$$\begin{aligned}
S_{\delta_2} &= \frac{128\pi}{45\delta^6 s^4 (\delta - z)(-2 + z)^{10} z^7 (\delta + z)} \left\{ \sqrt{\frac{z^2 - \delta^2}{(4 + \delta^2 - 4z)(1 - z)}} \right. \\
&\times [1843200\delta^{10}(4 + \delta^2)^2 z - 614400\delta^8(4 + \delta^2)(72 + 101\delta^2 + 15\delta^4)z^2 \\
&+ 30720\delta^6(10368 + 42816\delta^2 + 38368\delta^4 + 9574\delta^6 + 679\delta^8)z^3 \\
&- 5120\delta^6(390528 + 828736\delta^2 + 519596\delta^4 + 100453\delta^6 + 5487\delta^8)z^4 \\
&+ 5120\delta^4(-110592 + 1058144\delta^2 + 1531104\delta^4 + 744394\delta^6 + 115197\delta^8 + 4869\delta^{10})z^5 \\
&- 1280\delta^4(-2955264 + 6395328\delta^2 + 7124384\delta^4 + 2865924\delta^6 + 364442\delta^8 \\
&+ 11889\delta^{10})z^6 + 256\delta^2(1105920 - 43674880\delta^2 + 28767008\delta^4 + 26401544\delta^6 \\
&+ 9368320\delta^8 + 1006841\delta^{10} + 24907\delta^{12})z^7 - 64\delta^2(28139520 - 296599040\delta^2 \\
&+ 61689856\delta^4 + 44813600\delta^6 + 15834776\delta^8 + 1516544\delta^{10} + 27059\delta^{12})z^8 \\
&+ 32(-2949120 + 160276480\delta^2 - 617186304\delta^4 + 56704000\delta^6 + 10167648\delta^8 \\
&+ 7112432\delta^{10} + 718126\delta^{12} + 6753\delta^{14})z^9 + 16(47185920 - 527851520\delta^2 \\
&+ 729945600\delta^4 - 149188736\delta^6 + 13544832\delta^8 + 47360\delta^{10} - 144180\delta^{12} + 2483\delta^{14})z^{10} \\
&- 8(365363200 - 1046585344\delta^2 + 224047104\delta^4 - 415587456\delta^6 - 2576256\delta^8 \\
&+ 1710200\delta^{10} + 27764\delta^{12} + 635\delta^{14})z^{11} + 4(1772748800 - 990953472\delta^2 \\
&- 665257472\delta^4 - 664114560\delta^6 - 29465408\delta^8 + 277460\delta^{10} - 21175\delta^{12} + 210\delta^{14})z^{12} \\
&- 8(1473757184 + 199317504\delta^2 - 234019072\delta^4 - 150230864\delta^6 - 7587160\delta^8 \\
&- 124303\delta^{10} + 300\delta^{12})z^{13} - 4(-3491954688 - 1095510016\delta^2 + 45265792\delta^4 \\
&+ 71393200\delta^6 + 2794952\delta^8 - 18599\delta^{10} + 105\delta^{12})z^{14} - 4(2995691520 \\
&+ 946406400\delta^2 + 85150144\delta^4 - 3895992\delta^6 + 95674\delta^8 + 425\delta^{10})z^{15} \\
&+ 8(930959360 + 243791616\delta^2 + 24343872\delta^4 + 756392\delta^6 + 4617\delta^8)z^{16} \\
&- 96(34273280 + 6615552\delta^2 + 442968\delta^4 + 5637\delta^6)z^{17} \\
&+ 1024(956608 + 116158\delta^2 + 3367\delta^4)z^{18} - 16384(10698 + 631\delta^2)z^{19} + 14581760z^{20}] \\
&+ [1843200\delta^{12}(4 + \delta^2) - 614400\delta^{10}(72 + 89\delta^2 + 15\delta^4)z \\
&+ 61440\delta^8(1296 + 4228\delta^2 + 2819\delta^4 + 342\delta^6)z^2 \\
&- 15360\delta^8(25440 + 42856\delta^2 + 20593\delta^4 + 1869\delta^6)z^3 \\
&+ 7680\delta^6(-25344 + 104048\delta^2 + 120884\delta^4 + 48728\delta^6 + 3391\delta^8)z^4 \\
&- 3840\delta^6(-283392 + 218448\delta^2 + 197300\delta^4 + 78807\delta^6 + 4272\delta^8)z^5 \\
&+ 3840\delta^4(46080 - 725888\delta^2 + 107264\delta^4 + 74942\delta^6 + 44495\delta^8 + 1901\delta^{10})z^6
\end{aligned}$$

$$\begin{aligned}
& - 1920\delta^4(540672 - 2251264\delta^2 + 11080\delta^4 - 37482\delta^6 + 35347\delta^8 + 1209\delta^{10})z^7 \\
& + 480\delta^2(-98304 + 5812224\delta^2 - 9475072\delta^4 + 31856\delta^6 - 315944\delta^8 + 40476\delta^{10}) \\
& + 1147\delta^{12})z^8 - 480\delta^2(-540672 + 9385984\delta^2 - 7280768\delta^4 + 362224\delta^6 \\
& \quad - 179332\delta^8 + 9230\delta^{10} + 229\delta^{12})z^9 + 240\delta^2(-2670592 + 20128768\delta^2 - 8820608\delta^4 \\
& + 831568\delta^6 - 110696\delta^8 + 3933\delta^{10} + 85\delta^{12})z^{10} - 60\delta^2(-15597568 + 59650048\delta^2 \\
& - 18438144\delta^4 + 1779904\delta^6 - 84800\delta^8 + 2921\delta^{10} + 49\delta^{12})z^{11} + 30\delta^2(-30146560 \\
& + 61106176\delta^2 - 17407488\delta^4 + 980688\delta^6 - 26636\delta^8 + 640\delta^{10} + 7\delta^{12})z^{12} \\
& - 15\delta^2(-41222144 + 41398272\delta^2 - 13922048\delta^4 + 210896\delta^6 - 9404\delta^8 + 19\delta^{10})z^{13} \\
& - 15\delta^2(20840448 - 7954432\delta^2 + 4165888\delta^4 + 19040\delta^6 + 1242\delta^8 + 7\delta^{10})z^{14} \\
& + 15\delta^2(7962624 - 230400\delta^2 + 829440\delta^4 + 6508\delta^6 + 69\delta^8)z^{15} \\
& - 30\delta^2(1140736 + 139136\delta^2 + 48432\delta^4 + 219\delta^6)z^{16} + 240\delta^2(29312 + 4064\delta^2 \\
& + 321\delta^4)z^{17} - 1920\delta^2(488 + 41\delta^2)z^{18} + 61440\delta^2z^{19}] \\
& \times \ln \frac{z\sqrt{4 + \delta^2 - 4z} + 2\sqrt{(1-z)(-\delta^2 + z^2)}}{z\sqrt{4 + \delta^2 - 4z} - 2\sqrt{(1-z)(-\delta^2 + z^2)}}. \tag{37}
\end{aligned}$$

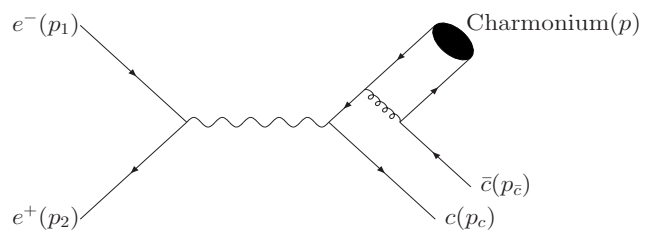
$$\begin{aligned}
\alpha_{\delta_2} &= \frac{128\pi}{45\delta^6 s^4(\delta - z)(-2 + z)^{10} z^7(\delta + z)} \left\{ \sqrt{\frac{z^2 - \delta^2}{(4 + \delta^2 - 4z)(1 - z)}} \right. \\
& \times [-614400\delta^{10}(4 + \delta^2)(4 + 3\delta^2)z + 614400\delta^8(96 + 164\delta^2 + 103\delta^4 + 15\delta^6)z^2 \\
& - 10240\delta^6(10368 + 47488\delta^2 + 39440\delta^4 + 17302\delta^6 + 2037\delta^8)z^3 \\
& + 5120\delta^6(124032 + 342400\delta^2 + 174148\delta^4 + 55779\delta^6 + 5487\delta^8)z^4 \\
& - 5120\delta^4(-55296 + 269984\delta^2 + 717792\delta^4 + 241766\delta^6 + 57183\delta^8 + 4869\delta^{10})z^5 \\
& + 1280\delta^4(-1480704 + 548416\delta^2 + 3899488\delta^4 + 895740\delta^6 + 153438\delta^8 + 11889\delta^{10})z^6 \\
& - 256\delta^2(-368640 - 21308160\delta^2 - 10322464\delta^4 + 18164600\delta^6 + 2826944\delta^8 \\
& + 319283\delta^{10} + 24907\delta^{12})z^7 + 64\delta^2(-19292160 - 131187200\delta^2 - 97682944\delta^4 \\
& + 49654496\delta^6 + 4871624\delta^8 + 221640\delta^{10} + 27059\delta^{12})z^8 \\
& - 32(2949120 - 186982400\delta^2 - 195251200\delta^4 - 189128192\delta^6 + 58393888\delta^8 \\
& + 3168624\delta^{10} - 155198\delta^{12} + 6753\delta^{14})z^9 - 16(-47185920 + 998072320\delta^2 \\
& - 51746304\delta^4 + 132896384\delta^6 - 73729792\delta^8 - 2617408\delta^{10} + 269788\delta^{12} \\
& + 2483\delta^{14})z^{10} + 8(-365363200 + 3412402176\delta^2 - 815620096\delta^4 - 165636992\delta^6 \\
& - 91975232\delta^8 - 2604552\delta^{10} + 185516\delta^{12} + 635\delta^{14})z^{11} - 4(-1772748800 \\
& + 8014970880\delta^2 - 1588918784\delta^4 - 462642816\delta^6 - 81292032\delta^8 - 1714116\delta^{10} \\
& + 24647\delta^{12} + 210\delta^{14})z^{12} + 8(-1473757184 + 3323742208\delta^2 - 346701568\delta^4 \\
& - 104122672\delta^6 - 10199336\delta^8 - 237265\delta^{10} + 3020\delta^{12})z^{13} - 4(-3491954688 \\
& + 3865319424\delta^2 - 63264896\delta^4 - 36776144\delta^6 - 2587160\delta^8 + 24425\delta^{10} \\
& + 105\delta^{12})z^{14} - 4(2995691520 - 1482234880\delta^2 - 56928320\delta^4 - 12344\delta^6 \\
& - 244390\delta^8 + 425\delta^{10})z^{15} + 8(930959360 - 150302976\delta^2 - 7609536\delta^4 \\
& - 529880\delta^6 + 4617\delta^8)z^{16} - 96(34273280 + 217600\delta^2 + 32792\delta^4 + 5637\delta^6)z^{17}
\end{aligned}$$

$$\begin{aligned}
& + 1024(956608 + 61294\delta^2 + 3367\delta^4)z^{18} - 16384(10698 + 631\delta^2)z^{19} \\
& + 14581760z^{20}] - [614400\delta^{12}(4 + 3\delta^2) - 614400\delta^{10}(24 + 31\delta^2 + 15\delta^4)z \\
& + 61440\delta^8(432 + 1604\delta^2 + 909\delta^4 + 342\delta^6)z^2 - 15360\delta^8(7968 + 19112\delta^2 \\
& + 5535\delta^4 + 1869\delta^6)z^3 + 7680\delta^6(-11520 + 21648\delta^2 + 68348\delta^4 + 9120\delta^6 \\
& + 3391\delta^8)z^4 - 3840\delta^6(-128256 - 39504\delta^2 + 165980\delta^4 + 5417\delta^6 + 4272\delta^8)z^5 \\
& + 3840\delta^4(39936 - 299136\delta^2 - 227520\delta^4 + 146914\delta^6 - 4783\delta^8 + 1901\delta^{10})z^6 \\
& - 1920\delta^4(491520 - 740864\delta^2 - 794120\delta^4 + 198970\delta^6 - 13267\delta^8 + 1209\delta^{10})z^7 \\
& + 480\delta^2(-98304 + 5386240\delta^2 - 1953792\delta^4 - 3425904\delta^6 + 424008\delta^8 - 30108\delta^{10} \\
& + 1147\delta^{12})z^8 - 480\delta^2(-442368 + 8620032\delta^2 - 530304\delta^4 - 2668784\delta^6 + 175028\delta^8 \\
& - 9350\delta^{10} + 229\delta^{12})z^9 + 240\delta^2(-1753088 + 17685504\delta^2 - 52352\delta^4 - 3219728\delta^6 \\
& + 102032\delta^8 - 2797\delta^{10} + 85\delta^{12})z^{10} - 60\delta^2(-7995392 + 48058368\delta^2 - 1542144\delta^4 \\
& - 6071104\delta^6 + 65680\delta^8 + 135\delta^{10} + 49\delta^{12})z^{11} + 30\delta^2(-11141120 + 43489280\delta^2 \\
& - 4092416\delta^4 - 4255696\delta^6 + 700\delta^8 + 632\delta^{10} + 7\delta^{12})z^{12} - 15\delta^2(-8323072 \\
& + 26431488\delta^2 - 3950848\delta^4 - 2012880\delta^6 - 5492\delta^8 + 173\delta^{10})z^{13} + 15\delta^2(196608 \\
& + 5984256\delta^2 - 673536\delta^4 - 272864\delta^6 - 182\delta^8 + 7\delta^{10})z^{14} - 15\delta^2(2064384 \\
& + 1408000\delta^2 + 93184\delta^4 - 13620\delta^6 + 69\delta^8)z^{15} + 30\delta^2(587776 + 184704\delta^2 \\
& + 24944\delta^4 + 219\delta^6)z^{16} - 240\delta^2(21632 + 4192\delta^2 + 321\delta^4)z^{17} \\
& + 1920\delta^2(440 + 41\delta^2)z^{18} - 61440\delta^2z^{19}] \\
& \times \ln \frac{z\sqrt{4 + \delta^2 - 4z} + 2\sqrt{(1-z)(-\delta^2 + z^2)}}{z\sqrt{4 + \delta^2 - 4z} - 2\sqrt{(1-z)(-\delta^2 + z^2)}} \}. \tag{38}
\end{aligned}$$

References

- [1] K.Hagiwara et al., Particle Data Group, Phys. Rev. D66, 010001 (2002).
- [2] Y.P.Kuang and T.M.Yan, Phys. Rev. D41, 155 (1990).
- [3] Y.B.Ding, D.H.Qin, and K.T.Chao, Phys. Rev. D44, 3562 (1991).
- [4] J.L.Rosner, Phys. Rev. D64, 094002 (2001).
- [5] E.Eichten et al., Phys. Rev. D21, 203 (1980); D17, 3090 (1978).
- [6] K.Heikkila et al., Phys. Rev. D29, 110 (1984).
- [7] W.Kwong and J.L.Rosner, Phys. Rev. D38, 279 (1988).
- [8] P.Moxhay, Phys. Rev. D37, 2557 (1988).
- [9] BES Collaboration, J.Z.Bai et al., hep-ex/0307028.
- [10] Y.P.Kuang, Phys. Rev. D65, 094024 (2002).
- [11] P. Wang, X.H. Mo, and C.Z. Yuan, hep/ph-0402227.

- [12] J.Z. Bai et al. (BES Collab.), Phys. Rev. D69, 012003(2004); Phys. Rev. Lett.92, 052001 (2004).
- [13] Belle Collaboration, K. Abe et al., hep-ex/0307061.
- [14] F.Yuan, C.F.Qiao, and K.T.Chao, Phys. Rev. D56, 329 (1997) (hep-ph/9701250).
- [15] P.W.Ko, J.Lee, and H.S.Song, Phys. Lett. B395, 107(1997) (hep-ph/9701235).
- [16] C.F.Qiao, F.Yuan, and K.T.Chao, Phys. Rev. D55, 4001 (1997) (hep-ph/9609284).
- [17] C.F.Qiao, F.Yuan, and K.T.Chao, Phys. Rev. D55, 5437 (1997) (hep-ph/9701249).
- [18] F.Yuan, C.F.Qiao, and K.T.Chao, Phys.Rev. D59, 014009 (1999) (hep-ph/9807329).
- [19] G.T. Bodwin, E. Braaten, and G. P. Lepage, Phys. Rev. D51, 1125 (1995).
- [20] P. Cho and K. Leibovich, Phys. Rev. **D 54**, 6690 (1996).
- [21] E. Braaten and Y.-Q. Chen, Phys. Rev. Lett. **76**, 730 (1996).
- [22] F. Yuan, C.F. Qiao, and K.T. Chao, Phys. Rev. **D 56**, 321 (1997); *ibid*, 1663 (1997).
- [23] S. Baek, P. Ko, J. Lee, and H.S. Song, J. Korean Phys. Soc. **33**, 97 (1998).
- [24] BaBar Collaboration, B. Aubert *et al.*, Phys. Rev. Lett. **87**,162002 (2001).
- [25] Belle Collaboration, K. Abe *et al.*, Phys. Rev. Lett. **88**, 052001(2002).
- [26] Belle Collaboration, K. Abe, *et al.*, Phys. Rev, Lett. **89**, 142001(2002).
- [27] E.Braaten and Jungil Lee, Phys. Rev. **D 67**, 054007 (2003); K.Y.Liu, Z.G.He and K.T.Chao, Phys. Lett. **B557**, 45 (2003); K.Hagiwara, E.Kou, and C.F.Qiao, Phys. Lett. **B570**, 39(2003).
- [28] K.Y.Liu, Z.G.He, and K.T.Chao, hep-ph/0301218, to appear in Phys. Rev. D.
- [29] E.J. Eichten and C. Quigg, Phys. Rev. **D52**, 1726 (1995).
- [30] E.Braaten, K.Cheung and T.C.Yuan, Phys. Rev. **D48**, 4230(1993).
- [31] T.C.Yuan, Phys. Rev. **D50**, 5664(1994); J.P.Ma, Phys. Rev. **D53**, 1185(1996).
- [32] K.Cheung and T.C.Yuan, Phys. Rev. **D53**, 3591(1996).
- [33] P.Cho and A.K.Leibovich, Phys. Rev. **D53**, (1996)6203; P.Cho and A.K.Leibovich, Phys. Rev. **D53**, (1996)150;
- [34] M.Beneke and M.Krämer, Phys. Rev. **D55**, (1997)5269.
- [35] G.T Bodwin et al., Phys. Rev. D46, 3703(1992).
- [36] L.Bergstrom and P. Ernstrom, Phys. Lett. B328, 153(1994).
- [37] M. Beneke et al., Phys. Rev. D59, 054003(1999).



+ 2 flipped graphs

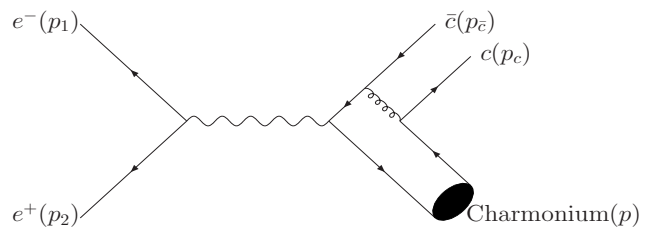
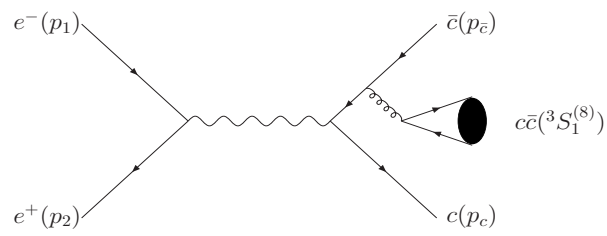


Figure 1: Feynman diagrams for $e^+ + e^- \rightarrow \gamma^* \rightarrow \text{charmonium} + c\bar{c}$.



+ 2 flipped graphs

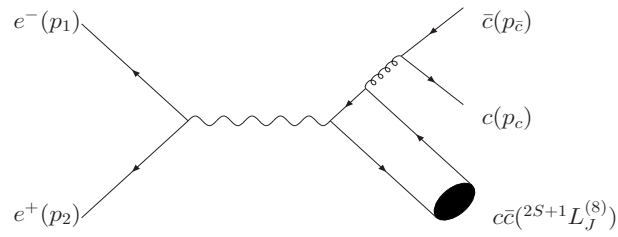


Figure 2: Feynman diagrams for $e^+ + e^- \rightarrow \gamma^* \rightarrow c\bar{c}({}^{2S+1}L_J^{(8)}) + c\bar{c}$.